

Supplementary Material

A modeling analysis of whole-body potassium regulation on a high potassium diet: Proximal tubule and tubuloglomerular feedback effects

Melissa M. Stadt¹ and Anita T. Layton^{1,2,3,4}

¹Department of Applied Mathematics, University of Waterloo, Waterloo, ON, Canada

²Cheriton School of Computer Science, University of Waterloo, Waterloo, ON, Canada

³Department of Biology, University of Waterloo, Waterloo, ON, Canada

⁴Department of Pharmacy, University of Waterloo, Waterloo, ON, Canada

1 Description of baseline mathematical model of potassium homeostasis regulation

Here we describe the mathematical model of potassium homeostasis used in our study. For more details on model development and parameter fitting see Stadt et al. [1]. A detailed model schematic is shown in Fig. S1. A list of the parameters and their values used in the baseline model is given in Table S2.

1.1 Internal K^+ balance

Internal K^+ is divided into 4 compartments: gastrointestinal and hepatoportal circulation (denoted by $M_{K_{gut}}$), plasma $[K^+]$ (denoted by K_{plasma}), interstitial fluid $[K^+]$ (K_{inter}), and intracellular $[K^+]$ (K_{IC}).

The amount of K^+ in the gut and hepatoportal circulation is given by

$$\frac{dM_{K_{gut}}}{dt} = 0.9 \times \Phi_{Kin} - k_{gut} \times M_{K_{gut}} \quad (S1)$$

where Φ_{Kin} is K^+ intake and k_{gut} is a parameter that determines how fast the K^+ is delivered to the plasma. Plasma $[K^+]$ concentration is given by

$$V_{plasma} \frac{dK_{plasma}}{dt} = k_{gut} \times M_{K_{gut}} - \Phi_{ECF} - \Phi_{uK} \quad (S2)$$

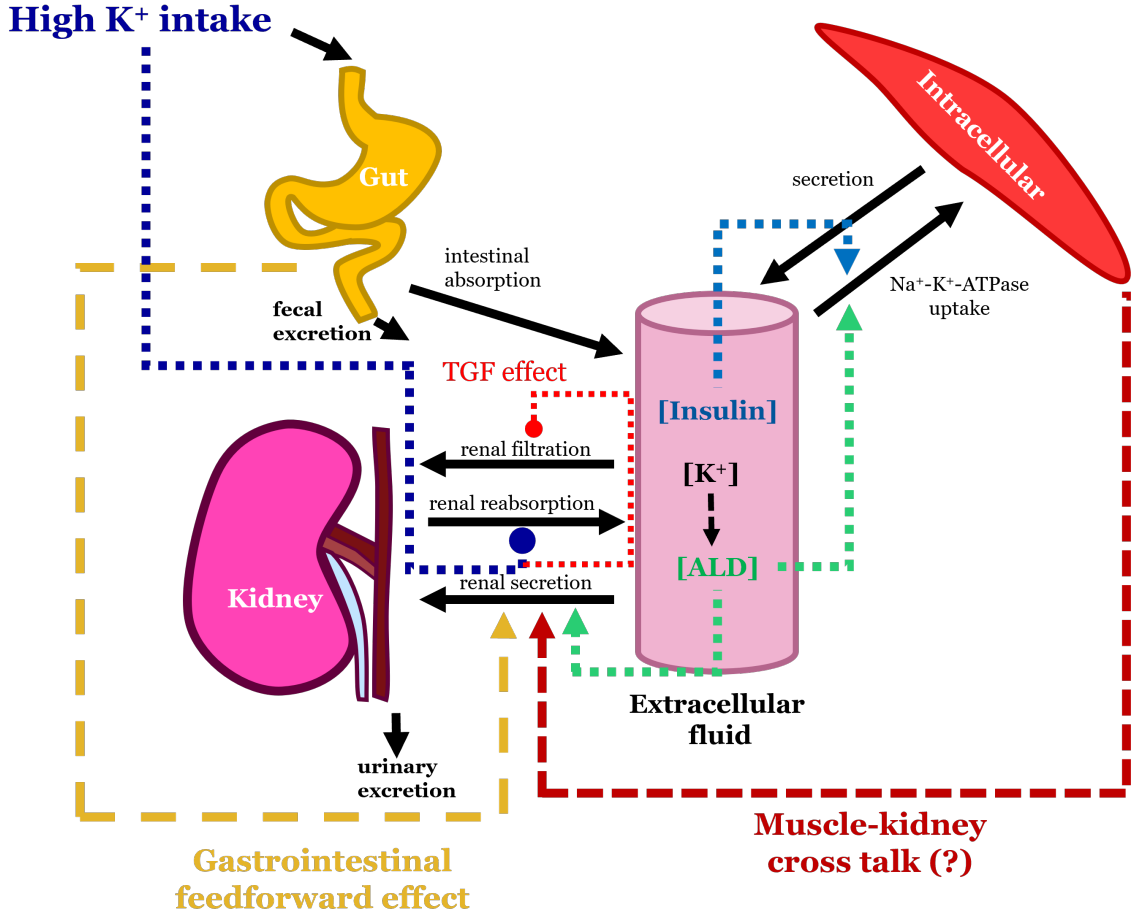


Figure S1: Detailed model schematic under high K^+ intake. Black arrows represent transport of K^+ between the compartments. Green, light blue, and yellow arrows represent the stimulating effects of aldosterone, insulin, and the gastrointestinal feedforward mechanism, respectively. High K^+ intake inhibitory effects on the proximal tubule (i.e., renal reabsorption) reabsorption is shown by the blunted dark blue arrow. Tubuloglomerular feedback (TGF) is shown by the blunted light red arrow. The hypothesized muscle-kidney cross talk signal is shown by the dark red arrow. The extracellular compartment is made up of plasma and interstitial fluid. ALD: aldosterone; TGF: tubuloglomerular feedback

where V_{plasma} is plasma volume, Φ_{uK} denotes urine K^+ excretion (described in Section 1.2); Φ_{ECF} denotes the diffusion of K^+ from the blood plasma to the interstitial space and is given by

$$\Phi_{\text{ECF}} = P_{\text{ECF}} \times (K_{\text{plasma}} - K_{\text{inter}}) \quad (\text{S3})$$

where P_{ECF} is a permeability parameter. Interstitial $[K^+]$ is determined by

$$V_{\text{inter}} \frac{dK_{\text{inter}}}{dt} = \Phi_{\text{ECF}} - \Phi_{\text{ECtoIC}} + \Phi_{\text{ICtoEC}} \quad (\text{S4})$$

where V_{inter} is the interstitial fluid volume, Φ_{ECtoIC} and Φ_{ICtoEC} are the fluxes of K^+ from the extracellular to the intracellular fluid and vice versa, respectively (see Eqs. S6 & S7). The intracellular $[K^+]$ is determined by the fluxes of K^+ in and out of the cells

$$V_{\text{IC}} \frac{dK_{\text{IC}}}{dt} = \Phi_{\text{ECtoIC}} - \Phi_{\text{ICtoEC}}. \quad (\text{S5})$$

Flow of K^+ into the intracellular fluid is driven by $Na^+-K^+-ATPase$ uptake and is modeled using Michaelis-Menten kinetics so that

$$\Phi_{ECtoIC} = \rho_{al} \times \rho_{insulin} \times \frac{V_{max} \times K_{inter}}{K_m + K_{inter}} \quad (S6)$$

where V_{max} is the maximum rate, K_m denotes the half maximal activation level, ρ_{al} is the effect of ALD on $Na^+-K^+-ATPase$ (see Section 1.3), and $\rho_{insulin}$ is the effect of insulin (see Section 1.4). K^+ returns to the extracellular compartment via diffusion through a permeable membrane:

$$\Phi_{ICtoEC} = P_{trans} \times (K_{IC} - K_{inter}) \quad (S7)$$

where P_{trans} denotes the transmembrane permeability.

1.2 Renal K^+ regulation

Filtered K^+ load (Φ_{filK}) is proportional to the GFR (Φ_{GFR}) and plasma $[K^+]$ so that

$$\Phi_{filK} = \Phi_{GFR} \times K_{plasma}. \quad (S8)$$

The filtrate then moves through the nephrons, where K^+ is reabsorbed and secreted along the different segments. At the end of the nephrons, what is remaining is excreted in urine. The model represents the kidney as a single nephron split into three segments: the “proximal segment (ps)” which includes the proximal tubule and the loop of Henle, the “distal segment (dt)” that includes the distal convoluted tubule and the connecting tubule, and the collecting duct (cd).

Let $\eta_{pt-Kreab}$ denote the fractional K^+ reabsorption along the proximal tubule. In normal K^+ intake this is about 67%. Fractional K^+ reabsorption along the loop of Henle is denoted by $\eta_{LoH-Kreab}$ and is about 25%. Therefore proximal segment reabsorption, denoted by $\eta_{ps-Kreab}$, is given by

$$\eta_{ps-Kreab} = \eta_{pt-Kreab} + \eta_{LoH-Kreab} \quad (S9)$$

so that net proximal segment K^+ reabsorption is given by

$$\Phi_{ps-Kreab} = \eta_{ps-Kreab} \times \Phi_{filK}. \quad (S10)$$

Distal tubule K^+ secretion is modeled using a baseline values of $\Phi_{dt-Ksec}^{eq}$ and is regulated by ALD and the gastrointestinal feedforward mechanism so that

$$\Phi_{dt-Ksec} = \Phi_{dt-Ksec}^{eq} \times \gamma_{al} \times \gamma_{Kin} \quad (S11)$$

where γ_{al} denotes the regulatory effect of ALD (see Section 1.3) and γ_{Kin} represents the gastrointestinal feedforward effect (see Section 1.5). Similarly, collecting duct K^+ secretion, denoted by $\Phi_{cd-Ksec}$, has a baseline value of $\Phi_{cd-Ksec}^{eq}$ and is regulated by ALD so that:

$$\Phi_{cd-Ksec} = \Phi_{cd-Ksec}^{eq} \times \lambda_{al} \quad (S12)$$

where λ_{al} denotes the regulatory effect of ALD (see Section 1.3). Collecting duct K^+ reabsorption ($\Phi_{cd-Kreab}$) is modeled as a linear function depending on the filtrate entering the collecting duct based transport from the previous segments:

$$\Phi_{cd-Kreab} = (\Phi_{filK} - \Phi_{ps-Kreab} + \Phi_{dt-Ksec}) \times A_{cd-Kreab} \quad (S13)$$

Urine K^+ excretion (Φ_{uK}) is given by the filtration and the net transport along the various segments:

$$\Phi_{uK} = \Phi_{filK} - \Phi_{ps-Kreab} + \Phi_{dt-Ksec} + \Phi_{cd-Ksec} - \Phi_{cd-Kreab}. \quad (S14)$$

1.3 Aldosterone effects

To model [ALD], denoted by C_{al} , we use the approach developed by Maddah & Hallow [2]:

$$C_{al} = C_{al}^{base} e^{m_K^{ALDO} \times (K_{ECF} - K_{ECF}^{base})} \quad (S15)$$

where m_K^{ALDO} is a fitting parameter and K_{ECF} is the extracellular $[K^+]$ given by

$$K_{ECF}^{total} = \frac{K_{plas} \times V_{plasma} + K_{inter} \times V_{inter}}{V_{plasma} + V_{inter}}$$

and $K_{ECF}^{baseline}$ is the baseline extracellular $[K^+]$. We capture the effect of [ALD] on $Na^+-K^+-ATPase$ abundance by the scaling factor ρ_{al} (see Eq. S6), which is represented linearly based on the findings of Phakdeekitcharoen et al. [3]:

$$\rho_{al} = \alpha_{al} + \beta_{al} \times C_{al} \quad (S16)$$

where α_{al} and β_{al} are parameters. The effect of [ALD] on distal tubule and collecting duct K^+ secretion are represented by γ_{al} and λ_{al} , respectively:

$$\gamma_{al} = A_{dt-Ksec} \times (C_{al})^{B_{dt-Ksec}} \quad (S17)$$

$$\lambda_{al} = A_{cd-Ksec} \times (C_{al})^{B_{cd-Ksec}} \quad (S18)$$

where $A_{dt-Ksec}$, $B_{dt-Ksec}$, $A_{cd-Ksec}$ and $B_{cd-Ksec}$ are parameters.

1.4 Insulin effects

The concentration of plasma insulin, denoted by $C_{insulin}$ in the time after a meal is given by

$$C_{insulin} = \begin{cases} \frac{(325-22.6) \text{ pmol/L}}{90 \text{ min}} \times (t - t_0 \text{ min}) + 22.6 \text{ pmol/L} & \text{if } t_0 \leq t < t_0 + 90 \\ \frac{-(325-22.6) \text{ pmol/L}}{270 \text{ min}} \times (t - (t_0 + 360 \text{ min})) + 22.6 \text{ pmol/L} & \text{if } t_0 + 90 \leq t \leq t_0 + 360 \\ 22.6 \text{ pmol/L} & \text{otherwise.} \end{cases} \quad (S19)$$

where t_0 is the time at the beginning of the meal.

To model insulin stimulation of $Na^+-K^+-ATPase$, we let $\rho_{insulin}$ (see (S6)) be given by a linear function bounded below by 1:

$$\rho_{insulin} = \max(1, A_{insulin} \times (C_{insulin} - C_{insulin}^{ss}) + 1) \quad (S20)$$

where $C_{insulin}^{ss} = 123.4 \text{ pmol/L}$ denotes steady state value for $C_{insulin}$ and $A_{insulin}$ is a fitting parameter. Note that due to how $C_{insulin}$ is formulated (Eq. S19), the maximal value for $\rho_{insulin}$ is given by

$$\rho_{insulin}^{max} = A_{insulin} (C_{insulin}^{max} - C_{insulin}^{ss}) + 1$$

where $C_{insulin}^{max} = 325 \text{ pmol/L}$ is the maximal value for $C_{insulin}$.

1.5 Gastrointestinal feedforward effect

The model represents gastrointestinal feedforward effect via the term γ_{Kin} , which alters distal tubule K^+ secretion depending on M_{Kgut} (see Eq. S11) where

$$\gamma_{Kin} = \max(1, A_{Kin} \times (M_{Kgut} - M_{Kgut}^{ss}) + 1) \quad (S21)$$

where A_{Kin} is a fitting parameter and M_{Kgut}^{ss} is the steady state value of M_{Kgut} .

1.6 Parameters

The model parameter values are given in Table S1 and ranges used in the Morris analysis are given in Table S2. Parameter fitting is discussed in Ref. [1].

Name	Unit	Original	Description
V_{plasma}	L	4.5	plasma volume
V_{inter}	L	10	interstitial volume
$V_{\text{intracellular}}$	L	24	intracellular volume
k_{gut}	min^{-1}	1.0e-2	K^+ delivery rate to plasma
P_{trans}	mmol/min	0.78	effective K^+ permeability from intracellular fluid
K_{m}	mmol/L	1.4	half maximal activation of NKATPase
V_{max}	mmol/min	130	maximum K^+ flow into cells
P_{ECF}	mmol/min	0.3	effective K^+ permeability in extracellular fluid
A_{Kin}	—	0.25	parameter that determined γ_{Kin}
$\Phi_{\text{GFR}}^{\text{base}}$	L/min	0.12	baseline glomerular filtration rate
$\eta_{\text{pt-Kreab}}^{\text{base}}$	—	0.67	baseline fractional PT reabsorption
$\eta_{\text{pt-Kreab}}$	—	0.36	fractional PT reabsorption (high K^+ diet)
α_{TGF}	ml/min	0.12	TGF parameter
$\eta_{\text{LoH-Keab}}$	—	0.25	loop of Henle fractional reabsorption
$\Phi_{\text{dt-Ksec}}^{\text{eq}}$	mmol/min	0.041	baseline distal tubule K^+ secretion
$A_{\text{dt-Ksec}}$	—	0.35	parameter that determines γ_{al}
$B_{\text{dt-Ksec}}$	—	0.24	parameter that determines γ_{al}
$\Phi_{\text{cd-Ksec}}^{\text{eq}}$	mmol/min	2.2e-3	baseline collecting duct K^+ secretion
$A_{\text{cd-Ksec}}$	—	0.16	parameter that determines λ_{al}
$B_{\text{cd-Ksec}}$	—	0.41	parameter that determines λ_{al}
$A_{\text{cd-Kreab}}$	—	0.50	parameter that determines $\Phi_{\text{cd-Kreab}}$
A_{insulin}	—	1.11	parameter that determines ρ_{insulin}
$K_{\text{IC}}^{\text{base}}$	mmol/L	130	baseline intracellular concentration
$K_{\text{ECF}}^{\text{base}}$	mmol/L	4.2	baseline extracellular concentration
$C_{\text{al}}^{\text{base}}$	ng/L	85	baseline ALD concentration
$m_{\text{K}}^{\text{ALDO}}$	—	0.5	parameter that determines C_{al}
α_{al}	—	0.74	parameter that determines ρ_{al}
β_{al}	—	3.04e-3	parameter that determined ρ_{al}

Table S1: Baseline parameter values and descriptions as used in the model simulations.

Name	Range	Original
k_{gut}	0.5e-2 - 1.5e-2	1.0e-2
A_{Kin}	0.13 - 0.38	0.25
$\Phi_{\text{GFR}}^{\text{base}}$	0.095 - 0.13	0.12
$\eta_{\text{pt-Kreab}}^{\text{base}}$	0.36 - 0.67	0.67
$\eta_{\text{pt-Kreab}}$	0.36 - 0.67	0.36
α_{TGF}	0.058 - 0.18	0.12
$\eta_{\text{LoH-Keab}}$	0.2 - 0.3	0.25
$\Phi_{\text{dt-Ksec}}^{\text{eq}}$	0.031 - 0.0672	0.041
$A_{\text{dt-Ksec}}$	0.17 - 0.52	0.35
$B_{\text{dt-Ksec}}$	0.12 - 0.36	0.24
$A_{\text{cd-Kreab}}$	0.3 - 0.75	0.50
A_{insulin}	0.27 - 0.82	0.55
$C_{\text{al}}^{\text{base}}$	42.5 - 127.5	85
$m_{\text{K}}^{\text{ALDO}}$	0.25 - 0.75	0.5
α_{al}	0.37 - 1.11	0.74
β_{al}	1.52e-3 - 4.6e-3	3.04e-3

Table S2: Parameter ranges and baseline values (from Ref. [1]) used for the Morris analysis. Parameters without a range given were not used in the Morris analysis. Parameter descriptions and units are the same as in Table S1.

2 Sensitivity analysis

2.1 Morris Method Description

Let f be a mathematical model where the output is given by $f(X_1, X_2, \dots, X_n)$ and X_1, X_2, \dots, X_n are the model inputs, which will be referred to as factors. When computing a sensitivity analysis using the Morris method, we start by determining a defined range for all the possible values for the factors. The factors are then rescaled to be uniformly distributed on the unit interval and an initial base value is selected at random from this distribution. Subsequently, one random factor, X_i , is incremented by a step size Δ , typically chosen to be $n/(2(n-1))$, where n is the number of factors. The elementary effect for the i -th factor, denoted by EE_i is computed by:

$$EE_i = \frac{f(X_1, X_2, \dots, X_i + \Delta, \dots, X_n) - f(X_1, X_2, \dots, X_i, \dots, X_n)}{\Delta}. \quad (\text{S22})$$

From this next value another random factor is incremented and the subsequent elementary effect is computed, until an elementary effect for each factor has been determined. This process is repeated r times by sampling at different points in the factor space. As a result, there will be a total of r elementary effects per factor at the end of the computations.

After computing the elementary effects for each factor, we can find the average value (μ_i), average of the absolute values (μ_i^*), standard deviation (σ_i), and Morris index (MI_i):

$$\begin{aligned} \mu_i &= \frac{\sum_{k=1}^r EE_i^k}{r} \\ \mu_i^* &= \frac{\sum_{k=1}^r |EE_i^k|}{r} \\ \sigma_i &= \sqrt{\frac{\sum_{k=1}^r (EE_i^k - \mu_i)^2}{r-1}} \\ MI_i &= \sqrt{(\mu_i)^2 + (\sigma_i)^2} \end{aligned}$$

where EE_i^k denotes the elementary effect of the i -th factor during the k -th model evaluation. The metrics can be interpreted in the following ways:

- The average of the absolute values, μ_i^* , gives a factor ranking: a greater μ_i^* value indicates that the i -th factor affects the model output.
- The standard deviation, σ_i indicates that this factor interacts with other factors or is nonlinear.
- The Morris index, MI_i is another way to factor rank by giving a single metric that incorporates both the mean (μ) and standard deviation (σ).

In an ordinary differential equation (ODE) model scenario, the factors are typically the model parameters. The model output measured can be the steady state solution, the values of the state variables at given time points in a simulation, or another measure that can be computed from a given model simulation (e.g., AUC in a PK model). In this study, the model output was the final plasma and intracellular $[K^+]$ after a 50 day simulation under high K^+ intake. The ranges for the parameters used in the Morris analysis are given in Table S2.

2.2 Muscle-kidney cross talk effects

In our previous study [1], we explored a hypothesized signal called “muscle-kidney cross talk” and predicted its effects under high and low K^+ intake. This signal is between intracellular fluid (driven by skeletal muscle) and kidneys, where the skeletal muscle intracellular $[K^+]$ directly affects urine K^+ excretion without changes in the extracellular $[K^+]$. In the same way as Ref. [1], muscle-kidney cross talk is not included in the baseline model because there has not been definitive evidence for this signal.

In this study, we further investigate the impacts of muscle-kidney cross talk in the context of a high K^+ diet by conducting “what-if” simulations, in addition to the baseline model simulations. The coupling function (ω_{Kic}) is taken to be a linearly increasing function of K_{IC} , bounded above 0:

$$\omega_{Kic} = \max(0, m_{Kic} (K_{IC} - K_{IC}^{\text{baseline}}) + 1). \quad (S23)$$

where the baseline value for $m_{Kic} = 0.1$. At homeostasis, $K_{IC} = K_{IC}^{\text{baseline}} = 145$ mEq/L, thus $\omega_{Kic} = 1$. To model a muscle-kidney cross talk signal that targets distal tubule K^+ secretion, we add the impact of ω_{Kic} by replacing the equation for distal segment K^+ secretion with

$$\Phi_{dt-Ksec} = \Phi_{dt-Ksec}^{\text{eq}} \times \gamma_{al} \times \gamma_{Kin} \times \omega_{Kic}. \quad (S24)$$

(We have previously found that the distal tubule target resulted in similar results to collecting duct reabsorption [1].)

Results for predicted intracellular $[K^+]$ during high K^+ diet simulations of muscle-kidney cross talk for varied m_{Kic} values with the PT + TGF effects are shown in Fig. S2A. A stronger cross talk signal, i.e., larger m_{Kic} , results in lower intracellular $[K^+]$ levels. When $m_{Kic} = 0.1$, intracellular $[K^+]$ levels remain within normal range for the full simulation. However, the predicted intracellular $[K^+]$ are on the high end of the normal range. Results for the same simulations with the addition of PT + TGF effects ($\eta_{pt-Kreab} = 0.36$ and $\alpha_{TGF} = \alpha_{TGF}^{\text{base}}$) are shown in Fig. S2B. We can see that with the PT + TGF effects and muscle-kidney cross talk parameter $m_{Kic} \geq 0.025$, intracellular $[K^+]$ levels remain within the normal range for the full simulation (Fig. S2B).

The intracellular and plasma $[K^+]$ at the end of the 50 day high K^+ simulations with and without PT + TGF effects for varied m_{Kic} are shown in Fig. S3. Regardless of PT + TGF effects, increasing m_{Kic} decreases both final intracellular and plasma $[K^+]$ levels (Fig. S3). As expected, adding the PT + TGF effects improved final intracellular and plasma $[K^+]$ levels. This is especially true for the no muscle-kidney cross talk simulation or small values of m_{Kic} . Final plasma $[K^+]$ levels are within normal range with the addition of the muscle-kidney cross talk for $m_{Kic} \geq 0.005$ (Fig. S3B), but final intracellular $[K^+]$ remains higher than normal range until $m_{Kic} \geq 0.025$ (Fig. S3A).

In summary, while the impacts of high K^+ intake on PT reabsorption greatly improve the model’s plasma and intracellular $[K^+]$ predictions, the presence of a muscle-kidney cross talk signal prevents excess K^+ from being stored in the intracellular fluid.

In our previous study [1], we used our mathematical model to conduct “what-if” simulations of muscle-kidney cross talk under short-term K^+ loading or depletion. Specifically, we found that in our baseline model (i.e., no muscle-kidney cross talk) after 4 days of K^+ loading (high K^+ intake), plasma $[K^+]$ levels started to reach hyperkalemic levels and intracellular $[K^+]$ levels remained high for several days after returning to normal K^+ intake [1]. When the muscle-kidney cross talk signal was included, model simulations predicted that intracellular $[K^+]$ levels remained within normal range. In this study, we extended our model to consider PT and TGF effects. Without the muscle-kidney cross talk signal, these effects were unable to keep both plasma and intracellular $[K^+]$ levels within normal ranges on a chronic high K^+ diet, which suggests that the muscle-kidney cross talk

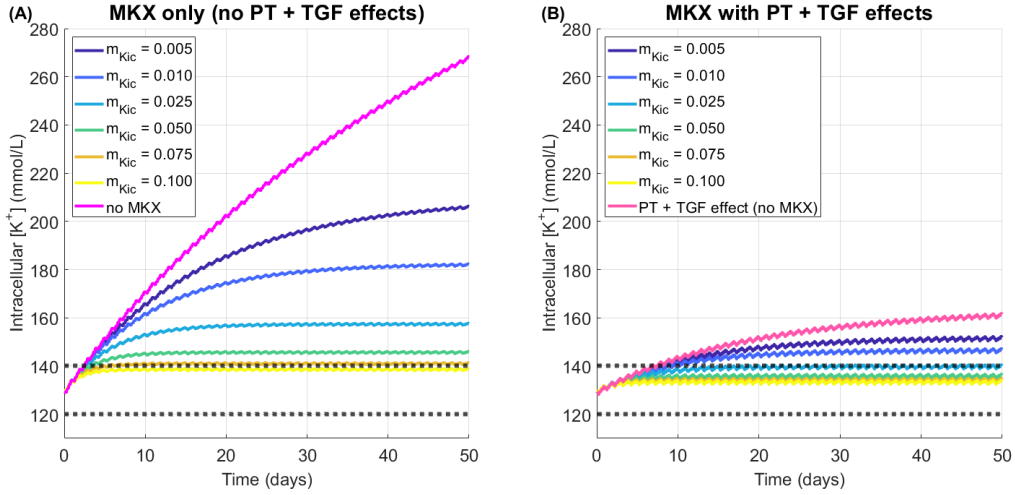


Figure S2: Model predictions of a high K^+ diet for 50 days with and without muscle-kidney cross talk (MKX) and proximal tubule and tubuloglomerular feedback effects (PT + TGF). PT + TGF effects includes the “TGF effect” (Eq. 2.2 in main text) with $\eta_{pt-Kreab} = 0.36$ as in Wang et al. [4] and α_{TGF} is the baseline value. (A) Model predictions of intracellular $[K^+]$ with muscle-kidney cross talk only where parameter m_{Kic} is the value as given by legend. (B) Model predictions of intracellular $[K^+]$ with muscle-kidney cross talk with PT + GFR high K^+ effects where parameter m_{Kic} is as given by the legend. Normal range for intracellular $[K^+]$ indicated by gray dotted line (120-140 mmol/L). MKX: muscle-kidney cross talk; PT: proximal tubule; TGF: tubuloglomerular feedback; m_{Kic} : muscle-kidney cross talk parameter (see Eq. S23).

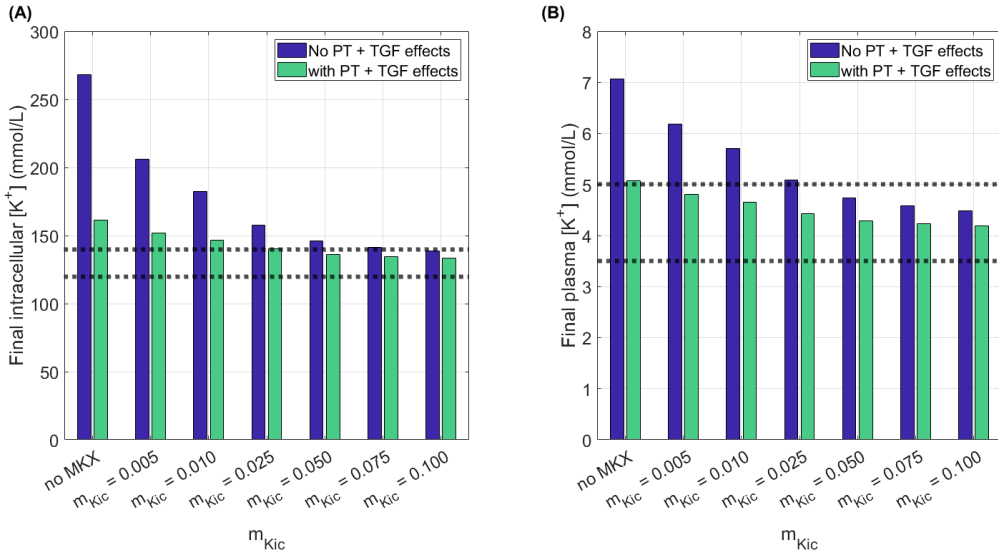


Figure S3: (A) Intracellular and (B) plasma $[K^+]$ levels at the end of 50 day simulation under with and without proximal tubule and tubuloglomerular feedback effects (PT + TGF effects). Muscle-kidney cross talk as given by the parameter m_{Kic} with or without PT + GFR effects. Normal ranges for intracellular and plasma $[K^+]$ indicated by gray dotted line (120-140 mmol/L and 3.5-5.0 mmol/L, respectively). PT: proximal tubule; TGF: tubuloglomerular feedback; m_{Kic} : muscle-kidney cross talk parameter (see Eq. S23).

signal may be one of the necessary regulatory mechanisms. To test this, we conducted “what-if” simulations of a high K^+ diet with varying strengths of the muscle-kidney cross talk signal (m_{Kic} ; Eq. S23). Model results indicated that muscle-kidney cross talk significantly improved K^+ balance (Fig. S2; Fig. S3).

References

- [1] Stadt MM, Leete J, Devinyak S, Layton AT. A mathematical model of potassium homeostasis: Effect of feedforward and feedback controls. *PLOS Computational Biology*. 2022 Dec;18(12):e1010607. Publisher: Public Library of Science. Available from: <https://journals.plos.org/ploscompbiol/article?id=10.1371/journal.pcbi.1010607>.
- [2] Maddah E, Hallow KM. A quantitative systems pharmacology model of plasma potassium regulation by the kidney and aldosterone. *Journal of Pharmacokinetics and Pharmacodynamics*. 2022 Jul. Available from: <https://link.springer.com/10.1007/s10928-022-09815-x>.
- [3] Phakdeekitcharoen B, Kittikanokrat W, Kijkunasathian C, Chatsudthipong V. Aldosterone increases Na⁺-K⁺-ATPase activity in skeletal muscle of patients with Conn's syndrome. *Clinical Endocrinology*. 2011;74(2):152-9. _eprint: <https://onlinelibrary.wiley.com/doi/pdf/10.1111/j.1365-2265.2010.03912.x>. Available from: <https://onlinelibrary.wiley.com/doi/abs/10.1111/j.1365-2265.2010.03912.x>.
- [4] Wang T, Liu T, Xu S, Frindt G, Weinstein AM, Palmer LG. High dietary K⁺ intake inhibits proximal tubule transport. *American Journal of Physiology-Renal Physiology*. 2023 Aug;325(2):F224-34. Publisher: American Physiological Society. Available from: <https://journals.physiology.org/doi/full/10.1152/ajprenal.00013.2023>.